DALTON
FULL PAPER

Synthesis and characterisation of chelating polycarboxylate ligands capable of forming intermolecular, complementary triple hydrogen bonds

Stefan Ulvenlund,[b] Alexandra S. Georgopoulou,[a] D. Michael P. Mingos,[a] Ian Baxter,[a] Simon E. Lawrence,[c] Andrew J. P. White[a] and David J. Williams[a]

[a] *Department of Chemistry, Imperial College of Science, Technology and Medicine, South Kensington, London, UK SW7 2AY*
[b] *Department of Explorative Pharmaceutics, Astra Draco AB, P.O. Box 34, S-22100 Lund, Sweden*
[c] *Department of Chemistry, University College Cork, Cork, Ireland*

The reaction between the dianhydride of ethylenedinitrilotetraacetic acid (edta) **1** and aminouracil derivatives was utilised to synthesize bifunctional, chelating ligands capable of co-ordinating to a metal centre *via* the edta backbone, while simultaneously being able to form complementary intermolecular hydrogen bonds *via* the uracil moieties. 5-Aminouracil **2**, 5-aminoorotic acid **3**, 5,6-diaminouracil **4** and 5,6-diamino-2-thiouracil **5** were treated with **1** in dry dmf or dmso to give functionalised dicarboxamide derivatives H_2L^1–H_2L^4 in 15–90% yield. The 5,6-diaminouracils **4** and **5** reacted with the dianhydride exclusively *via* the 5-amino position. The reaction of H_2L^1–H_2L^4 with basic metal salts [*e.g.* KVO_3 and $Zn(O_2CMe)_2$] in aqueous solutions led to the formation of metal complexes of the anionic ligands L^1–L^4: $K[VO_2L^1]\cdot 5H_2O$, $[Zn(OH_2)L^1]\cdot 4H_2O$ and $[Zn(OH_2)L^3]\cdot 5H_2O$ were characterized by single-crystal X-ray crystallography. The solid state structures of these complexes show that the uracil moieties are situated on pendant side-arms. The high degree of rotational freedom of these hydrogen-bonding groups makes this class of metal complex promising in terms of specific binding to water-soluble biomolecules having complementary hydrogen-bonding sites.

The precisely controlled formation of complex structures in nature is based on a range of recognition and self-association processes which depend on the shapes of the molecules and the specific interactions which occur between them. These interactions are often controlled by specific hydrogen-bonding interactions. The ability to mimic these systems using simpler organic molecules has led to the development and growth of supramolecular chemistry.[1] As a part of an ongoing project aimed at developing inorganic supramolecular chemistry, we have recently reported a number of ligands and metal complexes capable of forming intermolecular complementary triple hydrogen bonds and have shown that such systems may be used rationally to design metal-containing supramolecular aggregates in the solid state.[2] However, the compounds studied to date are generally insoluble in water. This drawback obviously inhibits investigations of molecular recognition phenomena involving these metal-based systems and water-soluble molecules displaying complementary hydrogen-bond sites, *e.g.* biomolecules. In an attempt to find water-soluble alternatives suitable for such applications, we have investigated functionalised polycarboxylate ligands. This paper describes the synthesis and characterisation of some of these compounds.

Amide condensation between amines and carboxylic acid anhydrides has previously been used to synthesize macrocycles,[3] functionalized ligands for pharmaceutical use (*e.g.* contrast agents for magnetic resonance imaging[4,5] and metal centres conjugated to antibodies)[6] and luminescent lanthanide complexes.[5] It appears, however, that this route has not been used previously to synthesize ligands suitable for applications within the realms of inorganic supramolecular chemistry and molecular recognition involving the formation of complementary hydrogen bonds. We have therefore used the reaction between the dianhydride of ethylenedinitrilotetraacetic acid (edta) **1** and a number of amino-substituted uracil derivatives **2**–**5** as a convenient route to functionalised, water-soluble chelating ligands

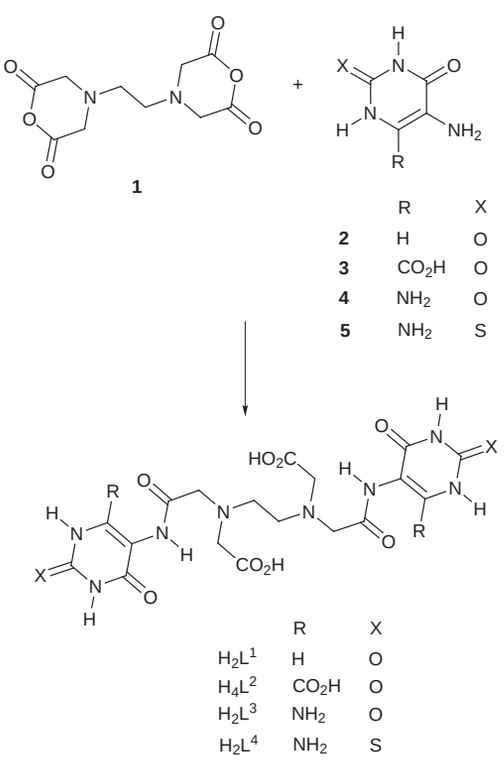

Scheme 1 The simple, one-step amino-deacyloxo route from the dianhydride of edta **1** to the diamides H_2L^1–H_2L^4. The diaminouracils **4** and **5** react with **1** in the 5-amino position only (see text). Note that H_4L^2 is a *tetra*-protic acid, due to the carboxylic acid group on the uracil moieties

with pendant groups capable of forming complementary hydrogen bonds (Scheme 1). The choice of uracil derivatives as the basis of the complementary hydrogen-bonding units arises

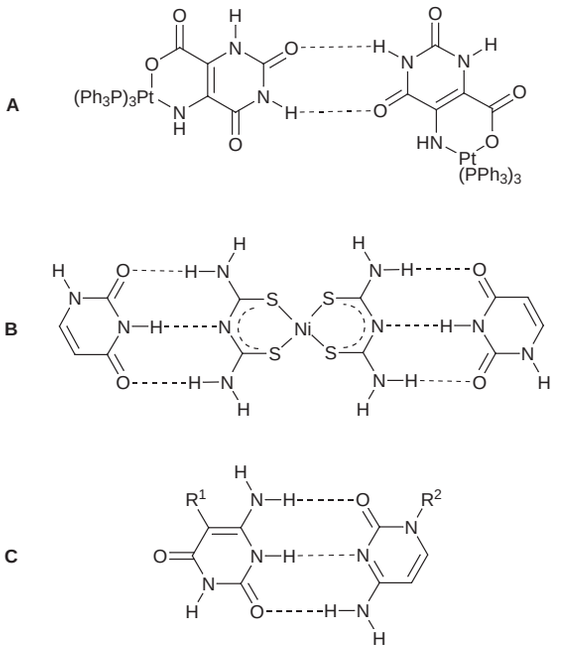

Scheme 2 Possible intermolecular hydrogen-bonding modes of uracil derivatives: (**A**) double AD–DA bonds as in the crystal structure of the tris(triphenylphosphine)platinum(II) complex of 5-aminoorotic acid **3**,[2] manifesting the self-complementarity of uracils; (**B**) triple ADA–DAD bonds as in the cocrystals of bis(dithiobiureto)nickel(II) and uracil;[7] and (**C**) triple DDA–AAD bonds between 6-aminouracil and cytosine derivatives, equivalent to those found in the cytosine–guanine base pairs in DNA

from the versatility of such moieties. Aminouracils have been shown to form at least three different types of complementary hydrogen bonds (Scheme 2): the double acceptor/donor–donor/acceptor (AD–DA) bonds observed in the crystal structure of $[Pt(PPh_3)_2L]$ (H_2L = 5-aminoorotic acid **3**);[2] the triple ADA–DAD bonds found in the cocrystals of bis(dithiobiureto)nickel(II) and uracil;[7] and, finally, the DDA–AAD bonds, which are analogous to the cytosine–guanine base pair in DNA.

Results and Discussion

Synthesis and characterisation of dicarboxamides H_2L^1–H_2L^4

The edta dianhydride **1** reacted with the aminouracil derivatives **2**–**5** in dry dmf or dmso to give the corresponding functionalised dicarboxamides, as outlined in Scheme 1. In the 5,6-diaminouracil derivatives, *e.g.* **4** and **5**, the 5-amino group is considerably more nucleophilic than the 6-amino group. Consequently, these bases reacted with the anhydride **1** only *via* the 5 position. After careful optimisation of the reaction conditions, the route generally gave high (virtually quantitative) yields of the crude products. The importance of selecting the right conditions was most dramatically displayed by H_2L^3 (the 5,6-diaminouracil derivative). The synthesis of this ligand proceeded in high yields in dmso, but was completely unsuccessful in dmf. The purification of the products tended to be cumbersome and wasteful due to their solubility characteristics, and consequently the overall yields of recrystallised, analytically pure products were only moderate. The yield of H_4L^2 was anomalously low (15%). This is probably due to the conjunction of the amine and carboxylic acid groups in the reacting base (5-aminoorotic acid **3**) and the resulting lowering of the nucleophilicity of the amino group.

The protonated ligands H_2L^1 through H_4L^4 are all soluble in dmf, dmso and hot water and sparingly or very sparingly soluble in cold water. They are insoluble in all other common organic solvents. Given these solubility characteristics, water is the only effective recrystallisation medium. Unfortunately, the compounds showed a marked tendency to supersaturate in this solvent and recrystallisation was, with the exception of H_2L^1, a slow and inefficient process. In addition, products isolated from the mother-liquor after prolonged standing were less pure than the initial products. This problem explains the relatively modest yields of the final, analytically pure products, which were generally isolated after cooling the aqueous recrystallisation solution with ice overnight. Attempts to circumvent the supersaturation problem by using water–acetone and –acetonitrile mixtures as recrystallisation media were largely unsuccessful since very large volumes of the solvent mixtures were required.

The most problematic (and enigmatic) solubility properties were displayed by H_4L^2. When freshly precipitated from the original reaction mixture in dmf (by adding chloroform) H_4L^2 was found to be very soluble in boiling water. However, after boiling for 30–90 min the product started to reprecipitate as its hydrate. Once isolated and dried this hydrate is almost insoluble in boiling water. A similar behaviour was displayed by H_2L^3, which although it dissolved in dmso in the original reaction mixture is only very sparingly soluble in this solvent after recrystallisation and drying. In stark contrast to their protonated analogues, the deprotonated ligands (*i.e.* the sodium, potassium and ammonium salts of L^1–L^4) are all exceedingly soluble in water.

The compounds H_2L^1, H_2L^3 and H_2L^4 are stable towards hydrolysis, but H_4L^2 is slowly hydrolysed to edta and 5-aminoorotic acid under reflux conditions. The low stability of H_4L^2 is presumably due to the conjugation of the amide bridge and the uracil moiety. Such a conjugation would also increase the acidity of the amide protons and may therefore account for the observation that H_4L^2 is the only dicarboxamide which does not display signals from these protons in the ^{1}H NMR spectrum. When dissolved in water or heated in air, H_2L^4 is susceptible to slow oxidation. This is evident from a slow yellow discoloration and a faint smell of SO_2. The reaction is, however, sufficiently slow to allow for both recrystallisation and complexation reactions to be performed using conventional open-bench techniques.

The compounds H_2L^1, H_4L^2 and H_2L^3 have sharp, well defined melting points (with decomposition), whereas H_2L^4 gradually decomposes without melting at temperatures >250 °C. The black residue has a melting point >350 °C.

Synthesis and characterisation of metal complexes of L^1, L^3 and L^4

Not surprisingly, the complexation properties of H_2L^1, H_2L^3 and H_2L^4 are very similar to those of edta. The complexation reactions are thus generally extremely easy to carry out. In the simplest cases the protonated ligands react with a stoichiometric amount of a water-stable, basic metal compound in aqueous solution to form the corresponding complex. The basic compound can be a carbonate [*e.g.* reaction (1)], a basic

$$H_2L + CaCO_3 \longrightarrow [CaL] + CO_2 + H_2O \qquad (1)$$

anion [*e.g.* reaction (2)], or even an oxide [*e.g.* reaction (3)].

$$H_2L + VO_3^- \longrightarrow [VO_2L]^- + H_2O \qquad (2)$$

$$H_2L + ZnO \longrightarrow [ZnL] + H_2O \qquad (3)$$

Owing to the comparatively weak basicity of the acetate ion, complexation reactions involving metal acetates $M(O_2CMe)_2$ were found to be less straightforward. For instance, whereas $Zn(O_2CMe)_2$ reacted smoothly with H_2L^1 to form the crystalline, neutral complex $[Zn(OH_2)L^1]$, $Cu(O_2CMe)_2$ and $Ni(O_2CMe)_2$ did *not* react with H_2L^1 in aqueous solutions, even after prolonged reflux. Instead, the complexes of Cu^{II} and Ni^{II} were synthesized by slow addition of the acetates to solutions of the ligands in aqueous KOH (see Experimental section).

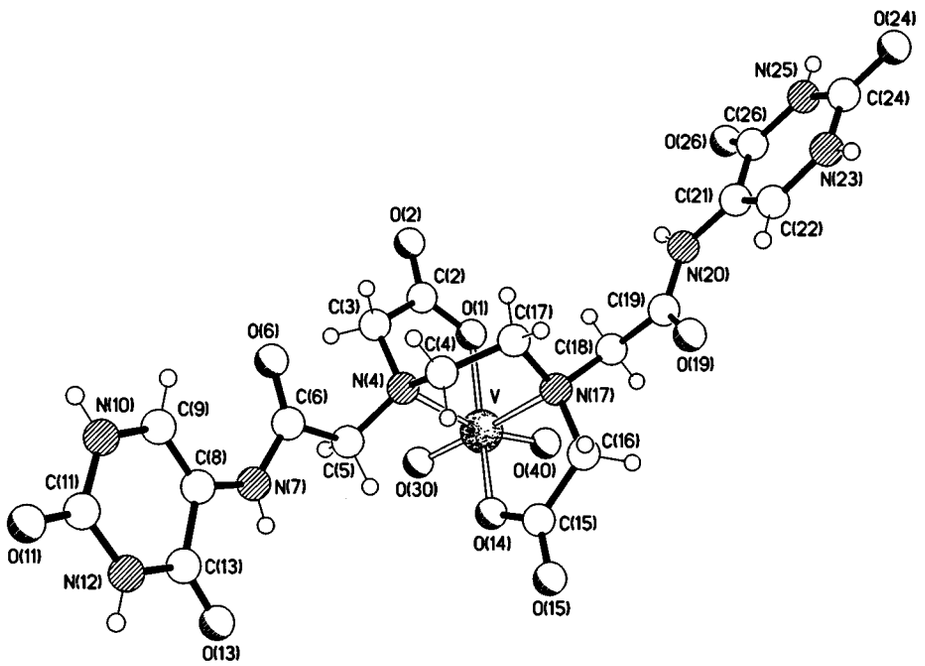

Fig. 1 Molecular structure of the anion in $K[VO_2L^1]\cdot 5H_2O$

Like the parent protonated ligands, the metal complexes tend to be soluble in polar solvents such as water, dmf and dmso. All complexation reactions were therefore carried out in aqueous solutions and the solid complexes isolated were invariably found to be hydrates. According to thermogravimetric analyses, the solid hydrates desolvate between 50 and 120 °C.

For a given metal ion, M^{2+}, the neutral complexes $[ML^1]$, $[ML^3]$ and $[ML^4]$ are very similar both in terms of the synthetic procedures used to make them and their properties. They are generally sparingly or very sparingly soluble in water. A notable exception in terms of solubility is $[CuL^1]$, which is exceedingly soluble. As would be expected, salts of anionic and cationic complexes are more water soluble than their neutral analogues. For example, $K[VO_2L^1]$ is soluble in cold water, whereas $[VOL^1]$ is virtually insoluble. The unwelcome tendency of the parent ligands to form supersaturated aqueous solutions (see above) is to a varying degree paralleled in the solubility properties of the complexes. For a given metal M this tendency generally increases in the series $[ML^1] < [ML^3] \ll [ML^4]$.

Like the parent protonated ligands, the complexes were insensitive to hydrolysis, even when aqueous solutions were refluxed for an extended period. However, an aerial oxidation process was noted for $[ML^4]$ complexes, which occurred in solution and upon heating under ambient conditions. Reflecting the behaviour of the parent ligand, this oxidation was sufficiently slow to allow the complexes to be conventionally handled in air temperatures below 100 °C. Complexation of the ligands increases their thermal stabilities substantially. Whereas H_2L^1 and H_2L^3 melt with decomposition below 300 °C, the corresponding complexes invariably have melting points above 360 °C. Complexes of H_2L^4 are, however, rapidly oxidised in air at temperatures above 150 °C.

Synthesis and characterisation of metal complexes of H_4L^2

Neutral $[M(H_2L^2)]$ complexes are generally very soluble in water, poorly crystalline and highly hydrated. These properties make them quite different from the analogous L^1, L^3 and L^4 complexes and this may be explained by the fact that H_4L^2 has four, rather than two, carboxylic acid groups. The additional carboxylate groups on the uracil moieties in L^2 may give rise to a 'co-ordinative ambiguity' of the ligand, since it is, in principle, possible for it to use both these groups *and* those on the edta backbone in complex formation. The ambiguity is emphasised by the fact that the uracil carboxylic acid groups are the most acidic ones, whereas chelation is probably more energetically favourable if co-ordination takes place *via* the edta backbone. With these structural ambiguities in mind, the co-ordination mode of the ligand in $[VO_2(H_2L^2)]^-$ was investigated by ^1H NMR spectroscopy. The CH_2 region of the spectrum of this species was found to be virtually identical to that of the structurally characterised analogue $[VO_2L^1]^-$ (see the next section), which strongly suggests that L^1 and H_2L^2 co-ordinate in an identical fashion to VO_2^+ and hence that the carboxylic acid groups on the uracil groups in H_2L^2 remain protonated in the complex.

Complexes of H_nL^2 are much less stable towards hydrolysis than the analogous complexes of L^1, L^3 and L^4. The rationalisation of this low stability is the same as that given above for free H_2L, *i.e.* a conjugation of the carboxamide bridge with the carboxylic acid groups.

Single-crystal structure of $K[VO_2L^1]\cdot 5H_2O$

The crystal structure analysis of $K[VO_2L^1]\cdot 5H_2O$ shows the ligand L^1 to be tetradentate, co-ordinating to the vanadium(v) centre in a manner reminiscent of edta complexes. The two central nitrogen atoms occupy *cis* positions and the carboxylates are monodentate and occupy *trans* positions. The remaining octahedral co-ordination sites are occupied by the two oxo ligands (see Fig. 1). The geometry at vanadium is severely distorted from idealised octahedral with angles in the ranges 75.4(1)–106.6(2) and 153.9(1)–164.0(2)° for pairs of *cis* and *trans* ligands. The largest departure from an ideal *cis* angle of 90° is for the pair of oxo ligands [106.6(2)°]. This is probably a consequence of (i) the mutual repulsion between the substantial electron densities in the two V=O bonds and (ii) the increased space provided by the narrow bite angles of the chelate. As a consequence, the vanadium atom is displaced towards each oxo ligand [O(30) and O(40)] relative to the plane of the four co-ordinated atoms normal to these directions by 0.28 and 0.30 Å respectively. The metal–ligand distances (Table 1) are comparable with those observed for the edta analogue.[8] The two carboxylate containing five-membered chelate rings are only slightly puckered with maximum deviations of 0.17 [N(4) to O(1)] and 0.13 Å [N(17) to O(14)] from their respective least-squares planes. The remaining portions of the tetradentate ligand have

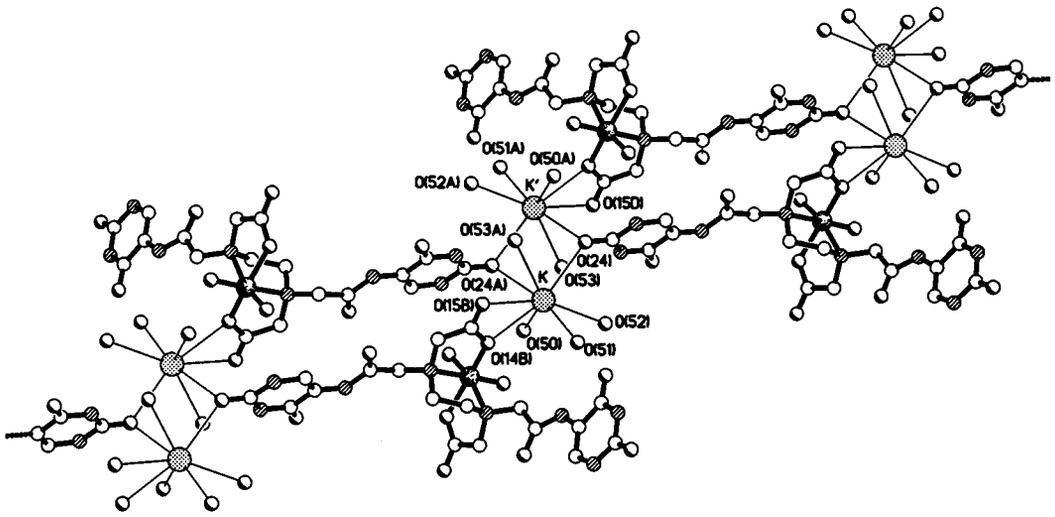

Fig. 2 Part of one of the stepped chains present in the structure of $K[VO_2L^1]\cdot 5H_2O$ showing the role of the potassium cations in chain formation. The shortest transannular K · · · K distance is 4.15 Å. The K–O distances are in the range 2.795(7) [O(51)] to 3.390(5) Å [O(15B)]

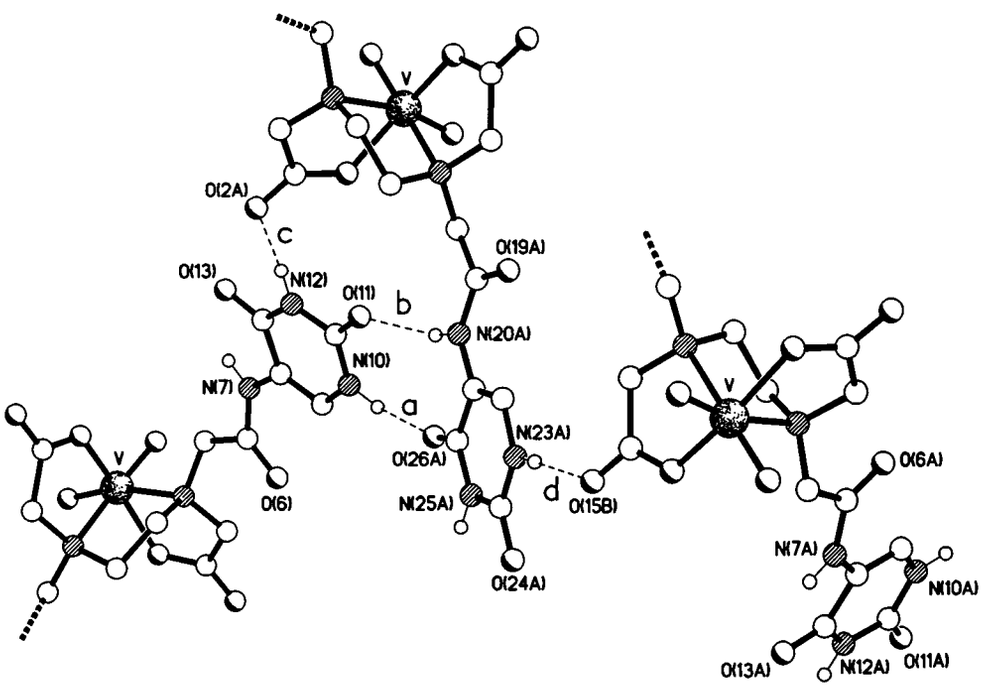

Fig. 3 Cross-linking of adjacent chains by N–H · · · O hydrogen bonding in the structure of $K[VO_2L^1]\cdot 5H_2O$. Hydrogen-bond geometries [N · · · O, H · · · O distances (Å) and N–H · · · O angles (°)]: **a**, 2.99, 2.15, 154; **b**, 2.82, 2.01, 150; **c**, 2.76, 1.87, 170; **d**, 2.81, 1.93, 166 (all N–H distances were normalised to 0.90 Å)

an extended geometry, the terminal oxygen atoms O(11) and O(24) being separated by 17.4 Å. The pendant uracil groups radiate in opposite directions from the edta–metal co-ordination sphere and the bond lengths and angles associated with these groups are similar to these reported for uracil derivatives.

The potassium counter cations occur in pairs in the structure (see Fig. 2) and are each co-ordinated to eight oxygen atoms. Each potassium ion co-ordinates to a pair of C_i related carbonyl oxygen atoms [O(24)] from bridging uracil moieties, and in a bidentate manner to one of the carboxylate groups [based on C(15)] of a third complex. The remaining four co-ordination sites are occupied by aqua ligands.* The combined effect of the potassium co-ordination is to create a stepped-chain polymeric structure that extends in the crystallographic *c* direction.

Adjacent chains are cross-linked *via* a pattern of N–H · · · O hydrogen bonds involving (i) the two uracil hydrogen atoms attached to N(10) and N(12) in one molecule, and a uracil carbonyl oxygen atom O(26) and a carboxylate oxygen atom O(2) of a second respectively (bonds **a** and **c** in Fig. 3), an interaction which is supplemented by a third N–H · · · O hydrogen bond involving the uracil carbonyl oxygen atom O(11) of the first molecule and the amide hydrogen atom attached to N(20) of the second (labelled **b** in Fig. 3), and (ii) the uracil hydrogen atom on N(23) of the second molecule and the carboxylate oxygen atom O(15) of a third (bond **d** in Fig. 3). The combination of the potassium co-ordination links and the N–H · · · O hydrogen bonding produces a continuous 'self-filling' three-dimensional network structure.

* Since the hydrogen atoms of both the potassium-co-ordinated aqua ligands and the included water molecule could not be located, no analysis of their possible involvement in hydrogen bonding is discussed.

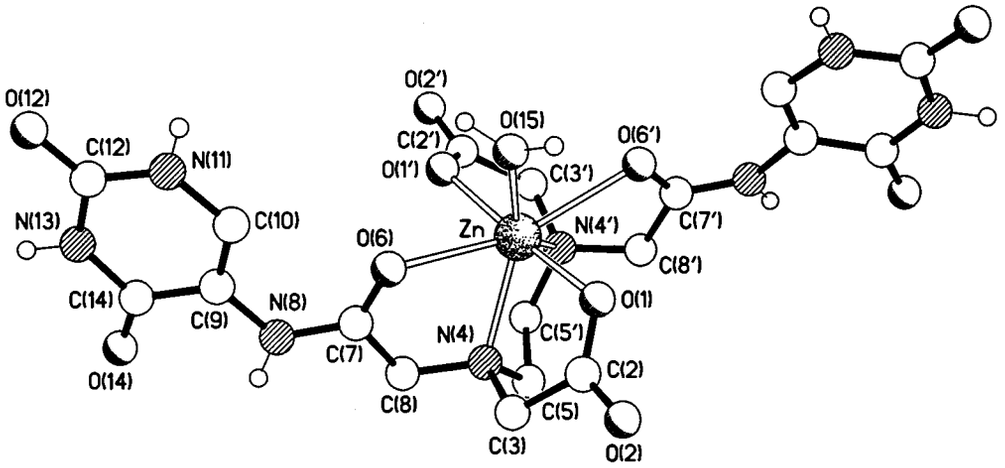

Fig. 4 Molecular structure of $[Zn(OH_2)L^1]\cdot 4H_2O$

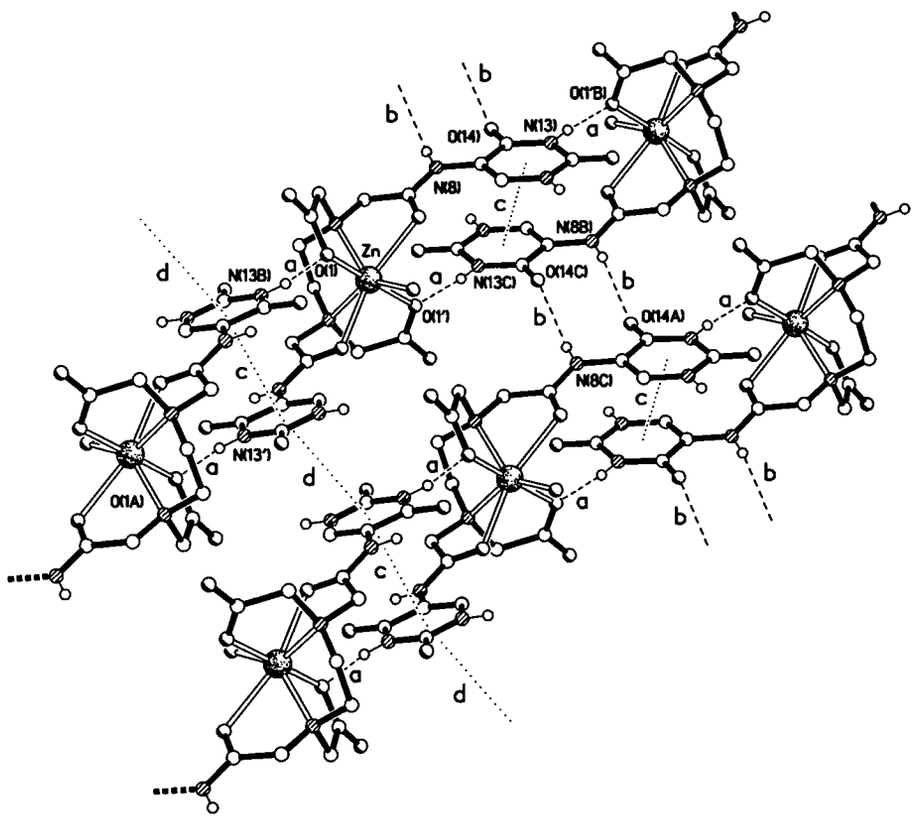

Fig. 5 Part of two adjacent chains of molecules present in the structure of $[Zn(OH_2)L^1]\cdot 4H_2O$, showing both the hydrogen bonding and ring stacking cross-linking between them. Hydrogen-bonding geometries [N · · · O, H · · · O distances (Å) and N–H · · · O angles (°)]: **a**, 2.80, 1.92, 167; **b**, 3.04, 2.28, 142 (all N–H distances were normalised to 0.90 Å). Ring-stacking interactions [mean interplanar and centroid · · · centroid separations (Å)]: **c**, 3.31, 3.56; **d**, 3.10, 4.07

Single-crystal structure of $[Zn(OH_2)L^1]\cdot 4H_2O$

The crystal structure of the complex formed between Zn^{2+} and L^1 shown in Fig. 4 has revealed a comparatively rare example of zinc with a co-ordination number of seven. Here, in contrast to $K[VO_2L^1]\cdot 5H_2O$, L^1 acts as a hexadentate ligand and the seventh co-ordination site is occupied by an aqua ligand. The co-ordination geometry can best be described as distorted monocapped trigonal prismatic, the aqua oxygen atom O(15) being the capping atom. The molecule has crystallographic C_2 symmetry about an axis passing along the Zn–OH_2 bond and bisecting the N–CH_2–CH_2–N linkage. The bond lengths (Table 2) differ significantly from those reported in related six-co-ordinate [Zn(edta)] complexes, which lie in the narrow range 2.0 to 2.2 Å.[9] In $[Zn(OH_2)L^1]\cdot 4H_2O$ the Zn–N distance is significantly longer at 2.248(3) Å whilst that to the amide oxygen atom O(6) is very much longer at 2.466(3) Å. The carboxylate- and amide-containing five-membered rings are puckered, with maximum deviations from planarity of 0.18 and 0.23 Å for the N(4) to O(1) and N(4) to O(6) chelates respectively. The uracil moieties once again are not involved in co-ordination to the zinc ions and function as radial pendant groups. The hexadentate co-ordination (*cf.* four-co-ordination in $K[VO_2L^1]\cdot 5H_2O$) produces a slight shortening of the length of the whole molecule, the terminal uracil oxygen atoms O(12) and O(12′) being separated by 15.2 Å.

Centrosymmetrically related pairs of molecules are linked 'end-to-middle' *via* N–H · · · O hydrogen bonds between one of the uracil N–H hydrogen atoms [on N(13)] of one molecule and one of the carboxylate oxygen atoms [O(1)] of the other (linkage **a** in Fig. 5) to form chains of molecules that extend in the crystallographic *c* direction. These hydrogen-bonding inter-

Table 1 Selected bond lengths (Å) and angles for $K[VO_2L^1]\cdot 5H_2O$

V–O(1)	1.977(3)	V–N(4)	2.387(4)
V–O(14)	1.990(3)	V–N(17)	2.373(4)
V–O(30)	1.635(3)	V–O(40)	1.619(3)
O(40)–V–O(30)	106.6(2)	O(40)–V–O(1)	96.1(2)
O(30)–V–O(1)	100.7(2)	O(40)–V–O(14)	99.8(2)
O(30)–V–O(14)	94.5(2)	O(1)–V–O(14)	153.9(1)
O(40)–V–N(17)	90.1(2)	O(30)–V–N(17)	162.0(2)
O(1)–V–N(17)	83.8(1)	O(14)–V–N(17)	75.6(1)
O(40)–V–N(4)	164.0(2)	O(30)–V–N(4)	88.5(2)
O(1)–V–N(4)	75.4(1)	O(14)–V–N(4)	84.0(1)
N(17)–V–N(4)	75.6(1)		

Table 2 Selected bond lengths (Å) and angles for $[Zn(OH_2)L^1]\cdot 4H_2O$

Zn–O(1)	2.094(3)	Zn–N(4)	2.248(3)
Zn–O(6)	2.466(3)	Zn–O(15)	2.005(5)
O(15)–Zn–O(1′)	86.8(1)	O(15)–Zn–O(1)	86.8(1)
O(1)–Zn–O(1′)	173.7(2)	O(15)–Zn–N(4′)	138.9(1)
O(1)–Zn–N(4′)	108.0(1)	O(15)–Zn–N(4)	138.9(1)
O(1)–Zn–N(4)	76.9(1)	N(4)–Zn–N(4′)	82.3(2)
O(15)–Zn–O(6′)	77.9(1)	O(1)–Zn–O(6′)	77.9(1)
N(4)–Zn–O(6′)	132.8(1)	O(15)–Zn–O(6)	77.9(1)
O(1)–Zn–O(6)	100.8(1)	N(4)–Zn–O(6)	68.7(1)
O(6)–Zn–O(6′)	155.8(2)		

Table 3 Selected bond lengths (Å) and angles for $[Zn(OH_2)L^3]\cdot 5H_2O$

Zn–N(1)	2.248(4)	Zn–N(4)	2.235(4)
Zn–O(6)	2.424(4)	Zn–O(9)	2.072(4)
Zn–O(12)	2.470(4)	Zn–O(15)	2.091(4)
Zn–O(29)	2.043(4)		
O(29)–Zn–O(9)	90.9(2)	O(29)–Zn–O(15)	91.2(2)
O(9)–Zn–O(15)	177.8(2)	O(29)–Zn–N(4)	141.0(2)
O(9)–Zn–N(4)	100.5(2)	O(15)–Zn–N(4)	77.5(2)
O(29)–Zn–N(1)	139.3(2)	O(9)–Zn–N(1)	77.5(2)
O(15)–Zn–N(1)	101.2(2)	N(4)–Zn–N(1)	79.7(2)
O(29)–Zn–O(6)	76.7(2)	O(9)–Zn–O(6)	104.2(2)
O(15)–Zn–O(6)	76.7(2)	N(4)–Zn–O(6)	134.1(1)
N(1)–Zn–O(6)	68.9(1)	O(29)–Zn–O(12)	78.2(2)
O(9)–Zn–O(12)	76.5(1)	O(15)–Zn–O(12)	103.6(2)
N(4)–Zn–O(12)	68.8(1)	N(1)–Zn–O(12)	134.0(1)
O(6)–Zn–O(12)	154.9(1)		

actions are supplemented by stacking interactions between the pairs of uracil rings (mean interplanar separation 3.31 Å, centroid · · · centroid separation 3.56 Å, **c** in Fig. 5). Adjacent chains are cross-linked by weak N–H · · · O hydrogen bonds (**b** in Fig. 5) between the amide hydrogen atom attached to N(8) in one chain and the uracil carbonyl oxygen atom O(14) in another, and by an extension of the stacking motif described above (**d** in Fig. 5). This latter stacking interaction is considerably weaker, the centroid · · · centroid separation being 4.07 Å. Additional cross-linking of the chains is provided by O–H · · · O hydrogen bonds involving both the aqua ligand[2] [O(15) · · · O(16) 2.73, H · · · O 1.85 Å, O–H · · · O 165°] and the water molecules of crystallisation [O(16) · · · O(2) 2.87, H · · · O 2.02 Å, O–H · · · O 155°; O(16) · · · O(14) 2.99, H · · · O 2.10 Å, O–H · · · O 172°; O(17) · · · O(2) 2.75, H · · · O 1.92 Å, O–H · · · O 151°; N(11) · · · O(17) 2.82, H · · · O 1.92 Å, N–H · · · O 176°]. Fig. 6 illustrates the slightly flattened 'close-packed hexagonal' arrangement of the hydrogen-bonded/stacked polymer chains, and shows the additional cross-linking roles played by the water molecules of crystallisation (broken bonds).

Single-crystal structure of $[Zn(OH_2)L^3]\cdot 5H_2O$

In the solid state structure of $[Zn(OH_2)L^3]\cdot 5H_2O$ shown in Fig. 7 all six donor sites on the edta backbone are co-ordinated to

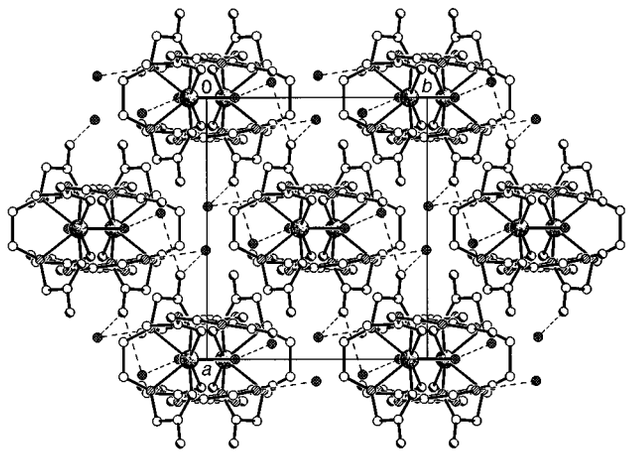

Fig. 6 'Hexagonal close-packed' arrangement of the hydrogen-bonded polymer chains in $[Zn(OH_2)L^1]\cdot 4H_2O$ showing the additional cross-linking involving the water molecules of crystallisation. The picture has been drawn in parallel projection looking down the crystallographic *c* direction

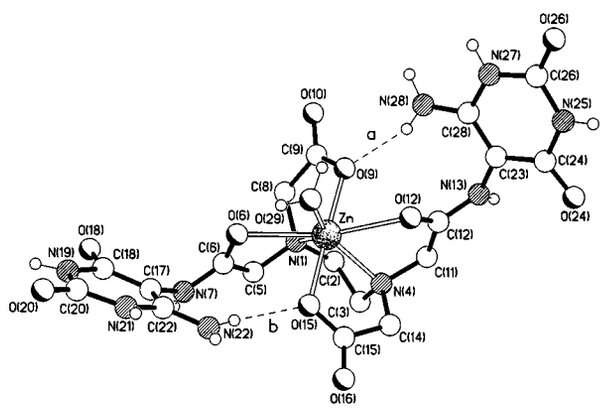

Fig. 7 Molecular structure of $[Zn(OH_2)L^3]\cdot 5H_2O$. Hydrogen-bonding geometries [N · · · O, H · · · O distances (Å) and N–H · · · O angles (°)]: **a**, 2.98, 2.14, 156; **b**, 2.94, 2.10, 156 (all N–H distances were normalised to 0.90 Å)

the central metal atom in an almost identical fashion to that observed in $[Zn(OH_2)L^1]\cdot 4H_2O$. Likewise, a seventh co-ordination site is occupied by an aqua ligand, O(29). The co-ordination polyhedron is again monocapped trigonal prismatic with Zn–O and Zn–N distances (see Table 3) that do not differ significantly from those observed in $[Zn(OH_2)L^1]\cdot 4H_2O$. However, the folding of the carboxyl containing five-membered rings is very much more pronounced than in either $K[VO_2L^1]\cdot 5H_2O$ or $[Zn(OH_2)L^1]\cdot 4H_2O$; the out-of-plane deviations range between 0.24 and 0.33 Å. Another major difference between the two zinc complexes is in the conformations of the extended ligand chains. In $[Zn(OH_2)L^1]\cdot 4H_2O$ (and also in $K[VO_2L^1]\cdot 5H_2O$) there is a near coplanarity of the amide groups with their associated uracil rings, whereas in $[Zn(OH_2)L^3]\cdot 5H_2O$ the uracil moieties are both steeply inclined. This latter orientation facilitates the formation of a pair of intracomplex N–H · · · O hydrogen bonds between the amino groups and their proximal co-ordinated carboxyl oxygen atoms (linkages **a** and **b** in Fig. 7). These interactions produce a shortening of the overall ligand length to 14.6 Å [O(20) to O(26)], *cf*. 17.4 and 15.2 Å in $K[VO_2L^1]\cdot 5H_2O$ and $[Zn(OH_2)L^1]\cdot 4H_2O$ respectively.

The complexes are linked head-to-tail *via* pairs of non-equivalent N–H · · · O hydrogen bonds between one of the uracil ring amido N–H atoms in one molecule and one of the uracil ring carbonyl oxygen atoms of a second (labelled **c** and **d** in Fig. 8) to form infinite chains. This hydrogen-bonding mode is very similar to that previously observed in the crystal structure of

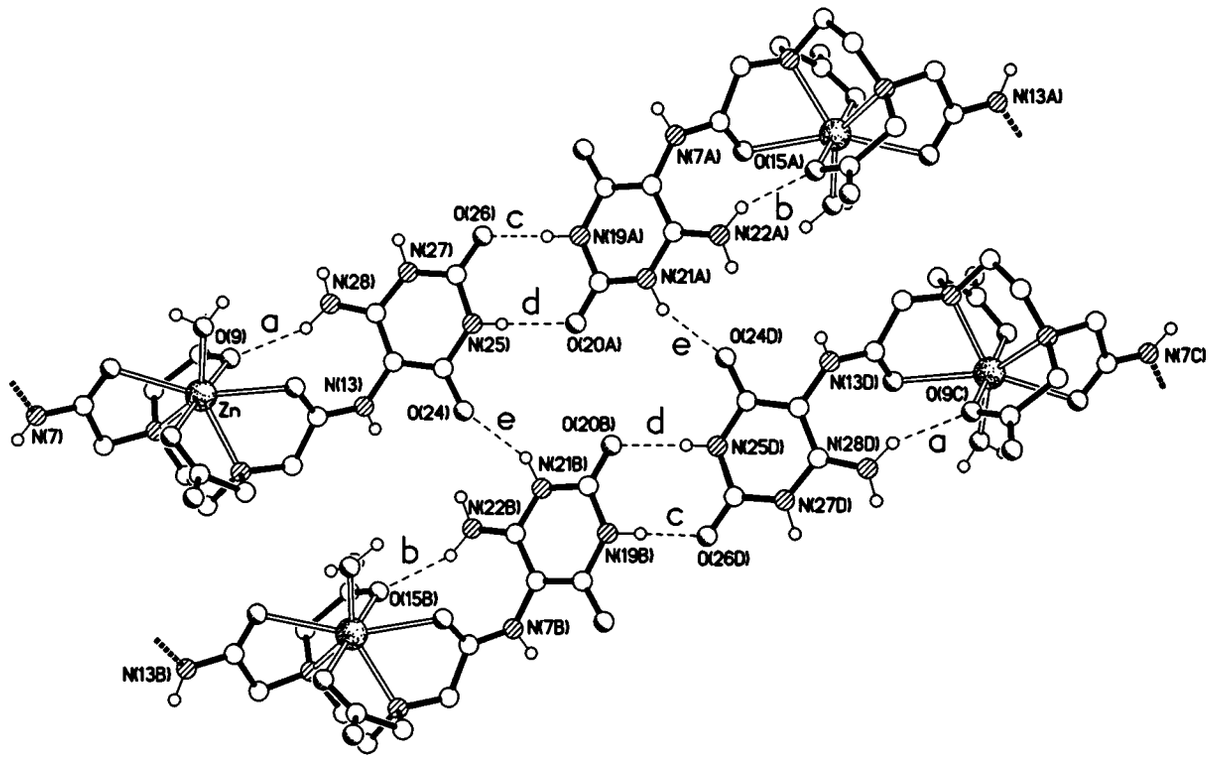

Fig. 8 Head-to-tail linking of uracil rings to form chains, and their cross-linking to form tapes, in the structure of $[Zn(OH_2)L^3]\cdot 5H_2O$. Hydrogen-bonding geometries [N···O, H···O distances (Å) and N–H···O angles (°)]: **c**, 2.76, 1.88, 175; **d**, 2.97, 2.07, 173; **e**, 2.87, 2.05, 150 (all N–H distances were normalised to 0.90 Å)

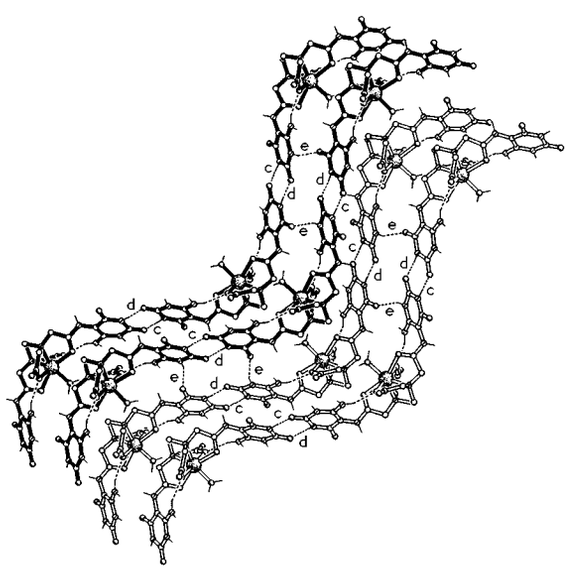

Fig. 9 Part of one of the ruckled sheets formed by the cross-linked sinuous tapes present in the structure of $[Zn(OH_2)L^3]\cdot 5H_2O$. The heavy bonds depict an extension of the partial tape shown in Fig. 8

$[Pt(PPh_3)_2L]$ (H_2L = 5-aminoorotic acid **3**).[2] Adjacent chains are cross-linked to form tapes *via* additional N–H···O hydrogen bonds between neighbouring uracil ring systems (linkage **e** in Fig. 8).

These tapes are sinuous in nature and extend along the crystallographic 201 direction. Each tape is twisted such that in certain regions the adjacent end-linked uracil rings are oriented side-to-side whereas in others they are stacked one above the other (though the mean interplanar separation of 3.92 Å precludes any significant stacking interactions). The overall assemblage of cross-linked tapes produces the highly ruckled sheet superstructure shown in Fig. 9. These sheets are cross-linked *via* O–H···O hydrogen bonds involving the intercalated water molecules with O···O distances ranging between 2.69 and 2.90 Å.

Complexes of L^1–L^4 in a supramolecular context

In terms of supramolecular chemistry, the most noteworthy feature revealed in the single crystal structures of $[VO_2L^1]^-$, $[Zn(OH_2)L^1]$ and $[Zn(OH_2)L^3]$ is that the uracil groups which are capable of forming three complementary hydrogen bonds are situated on pendant side arms (Figs. 1, 4 and 7). These side arms would be expected to have a high degree of rotational freedom in solution and thus a capacity to adapt to different environments. This suggests that the complexes have a potential to form selective, intermolecular hydrogen bonds with complementary molecules without this necessarily having a predictable orientational effect on the complex as a whole. This is a completely different situation compared to the complexes previously reported by our research group, where the hydrogen-bonding moieties are rigid with respect to the complex as a whole.[1,2] In terms of crystal engineering (where the ultimate goal is to control the exact way in which molecules or ions pack in the solid state) such a rigidity is, of course, desirable, since it lowers the number of possible configurations of the complex. However, in terms of selective binding to bio- and macromolecules the rigidity may be a drawback. The flexibility of ligands such as L^1 and L^3 can prove to be an advantage since it allows for the complex to adapt to the binding site. Experimental and molecular modelling studies of the interactions between these and related complexes and biomolecules are currently being made.

More generally this research has demonstrated that it is possible to incorporate on to the surface of edta complexes pendant groups which have the potential to form specific interactions *via* hydrogen bonds with bioactive molecules. Since edta complexes have been widely used in biological chemistry either as imaging agents or in a pharmaceutical role these complexes are potentially very interesting.

Experimental

Chemicals, general procedures and data collection

Ethylenedinitrilotetraacetic dianhydride [4,4′-ethylenebis-(morpholine-2,6-dione)] **1**, 5-aminouracil (5-amino-2,4-dihydroxypyrimidine) **2**, 5-aminoorotic acid (5-amino-2,6-dihydroxypyrimidine-4-carboxylic acid) **3** and 5,6-diamino-3-thiouracil (4,5-diamino-6-hydroxy-2-sulfanylpyrimidine) **5** were purchased from Aldrich Chemicals. Compound **1** was used as received, whereas **2**, **3** and **5** were dried at 100 °C for several days prior to use. 5,6-Diaminouracil (5,6-diamino-2,4-dihydroxypyrimidine) **4** was purchased from Sigma Chemicals as its hemisulfate salt. The free base was obtained by dropwise addition of an equimolar amount of aqueous KOH (0.053 M) to a slurry of the hemisulfate in water (5 g in 30 cm^3). After separation by filtration, the free base was dried at 150 °C under vacuum for 8 h. Ammonium metavanadate (NH_4VO_3, Aldrich, 99%) and zinc diacetate dihydrate (Aldrich, 98%) were used as received; dmf and dmso were distilled from BaO under reduced pressure just prior to use.

The reactions between compounds **1** and **2**–**5** were carried out under nitrogen. Subsequent purifications and manipulations of the products were carried out under ambient conditions with solvents which were used as received. The IR spectra (resolution 4 cm^{-1}) were recorded on a Perkin-Elmer 1720 spectrometer as KBr pellets, ^{1}H NMR spectra on a JEOL JNM-EX270 spectrometer operating at a ^{1}H frequency of 270 MHz and ^{1}H-decoupled ^{13}C NMR spectra on a JEOL JNM-EX270 spectrometer operating at a ^{13}C frequency of 67 MHz or a Bruker DRX-400 spectrometer operating at 100 MHz. All NMR samples were dissolved in $(CD_3)_2SO$ and all chemical shifts given relative to $SiMe_4$. Microanalyses were carried out by the Imperial College Microanalytical Service or by the Microanalytical Laboratory at University College of London.

Synthesis of the ligands

H_2L^1. Compounds **1** (2.00 g, 7.80 mmol) and **2** (2.20 g, 17.3 mmol) were added to dmf (80 cm^3) and left for 27 h at 90 °C with vigorous stirring. After cooling to room temperature, acetone (400 cm^3) was added to the thick, cream colored slurry and the system left for 30 min with continuing stirring. The product was isolated by filtration and washed with acetone (2 × 40 cm^3). After drying at 100 °C for 4 d at normal pressure, anhydrous H_2L^1 was obtained as a white, non-crystalline powder (3.66 g, 92% based on **1**), m.p. 235–237 °C (decomp.) (Found: C, 42.1; H, 4.5; N, 21.7%; $M - H^+$ *m/z* 509. $C_9H_{11}N_4O_5$ requires C, 42.4; H, 4.3; N, 21.9%; *M* 510). $\tilde{\nu}_{max}/cm^{-1}$ (CO) 1724vs and 1679vs; (amide I) 1639vs; (amide II) 1552s; (amide III) 1240m; δ_H(270 MHz) 2.86 (4 H, s, NCH_2CH_2N), 3.44 (4 H, s, NCH_2CONH), 3.51 (4 H, s, NC$H_2$$CO_2$H), 8.19 (2 H, d, ^3J 5.5, uracil CH), 9.35 (2 H, s, NCH_2CO), 10.74 (2 H, dd, ^3J 5.5, ^4J 1.5, CHN*H*CO), 11.60 (2 H, d, ^3J 5.5 Hz, CONHCO) and 12.5 (2 H, br s, CO_2H); δ_C(67 MHz) 56.4 (N*C*H_2*C*H_2N), 58.9 (N*C*H_2CONH), 62.4 (N*C*$H_2$$CO_2$H), 117.0 (uracil C5), 131.4 (uracil C6), 153.5 (uracil C2), 164.4 (uracil C4), 173.4 (NCH_2*C*ONH) and 176.2 (NCH_2*C*O_2H); *m/z* 509 ($M - H^+$).

H_4L^2. Compounds **1** (1.00 g, 3.90 mmol) and **3** (1.45 g, 8.47 mmol) were added to dmf (40 cm^3) and stirred at 60 °C. After 19 h the dark slurry was filtered, yielding a greenish brown eluate and a green solid. The latter was confirmed as being unchanged 5-aminoorotic acid by IR spectroscopy. To the eluate was added chloroform (100 cm^3), which caused the precipitation of an off-white, waxy solid. The system was stirred for 10 min and then filtered. The crude product (still somewhat wet) was transferred to boiling water (30 cm^3). Initially, all the solid dissolved forming a brown solution, but after *ca*. 15 min recrystallisation of the hydrated product in the form of a white solid commenced. After 35 min the reflux was discontinued and the product isolated by filtration, without allowing the temperature of the system to drop below 90 °C. The filtrate was dried at 100 °C for 1 h and then at 65 °C for 3 d, which yielded the tetrahydrate of H_4L^2 as an off-white powder (0.40 g, 15% based on **1**), m.p. 210–212 °C (Found: C, 35.7; H, 4.4; N, 16.5%; $M - H^+$ *m/z* 597. $C_{10}H_{11}N_4O_7 \cdot 4H_2O$ requires C, 35.8; H, 4.5; N, 16.7%; *M* 598). $\tilde{\nu}_{max}/cm^{-1}$ (CO) 1717vs; (amide I) 1679vs; (amide II) 1560m; (amide III) 1295m; δ_H(270 MHz) 2.99 (4 H, s, NCH_2-CH_2N), 3.63 (4 H, s, NCH_2CO), 3.66 (4 H, s, NC$H_2$$CO_2$H), ≈5 (vbr s, amide NH and CO_2H), 10.73 [2 H, s, C(CO_2H)N*H*CO] and 11.44 (2 H, s, CON*H*CO); δ_C(100 MHz) 51.2 (N*C*H_2-*C*H_2N), 54.4 (N*C*H_2CONH), 56.6 (N*C*$H_2$$CO_2$H), 109.6 (uracil C5), 139.0 (uracil C6), 149.2 (uracil C2), 161.6 (uracil C4), 161.9 (CO_2H on uracil moiety), 168.7 (NCH_2*C*ONH) and 171.3 (NCH_2*C*O_2H); *m/z* 597 ($M - H^+$).

H_2L^3. Compounds **1** (2.80 g, 10.9 mmol) and **4** (3.09 g, 21.8 mmol) were added to dmso (60 cm^3) and stirred at 70 °C under nitrogen (this reaction is *not* possible to perform in dmf). The material rapidly dissolved and a dark orange-green solution was obtained. After 75 min the temperature was lowered to 40 °C and the reaction allowed to continue for 20 h. After filtering the reaction mixture, the crude product was precipitated by adding acetone (1000 cm^3) and the slurry stirred for 90 min before being filtered again. In order to remove more of the retained dmso, the product was slurried in acetone (200 cm^3) for 25 min and then isolated by a third filtration. It was next transferred to boiling water (120 cm^3). It initially dissolved, but within minutes started to recrystallise. The cloudy solution was cooled on ice for 1 h and then filtered. The isolated light green solid was washed with acetone (100 cm^3) before being dried at 100 °C for 2 h. More crude product was obtained from the eluate from the last filtration by evaporating it under reduced pressure until 50 cm^3 remained and letting it stand at room temperature for 3 d. The precipitated crude yellow product was likewise isolated by filtration, washed with acetone (40 cm^3) and dried in an oven at 100 °C. Next, both fractions of the crude product were mixed and recrystallised a final time from boiling water (3500 cm^3). When a clear green solution was obtained the system was filtered and then evaporated at boiling point until *ca*. 2000 cm^3 remained (at which point recrystallisation commenced). After standing at room temperature for 2 d the final product was isolated by filtration, washed with water (150 cm^3) and acetone (150 cm^3). After drying at 100 °C at ambient pressure for 3 d the hydrate of H_2L^3 was isolated as a very pale green powder (2.82 g, 46% based on **1**), m.p. 294–296 °C (Found: C, 38.2; H, 4.8; N, 24.9%; $M - H^+$ *m/z* 539. $C_{18}H_{24}N_{10}O_{10} \cdot 1.5H_2O$ requires C, 38.1; H, 4.8; N, 24.7%; *M* 540). $\tilde{\nu}_{max}/cm^{-1}$ (CO) 1719vs, 1693vs and 1676vs; (amide I) 1624vs; (amide II) 1515m; (amide III) 1246m; δ_H(270 MHz) 2.99 (4 H, s, NCH_2CH_2N), 3.52 (4 H, s, NCH_2CO), 3.59 (4 H, s, NC$H_2$$CO_2$H), 6.27 (4 H, s, NH_2), 8.56 (2 H, s, amide NH), 10.39 [2 H, s, C(NH_2)-N*H*CO] and 10.51 (2 H, s, CON*H*CO); δ_C(67 MHz) 51.8 (N*C*H_2*C*H_2N), 55.5 (N*C*H_2CONH), 57.1 (N*C*$H_2$$CO_2$H), 86.2 (uracil C5), 149.7 (uracil C6), 151.3 (uracil C2), 161.4 (uracil C4), 170.3 (NCH_2*C*ONH) and 172.0 (NCH_2*C*O_2H); *m/z* 539 ($M - H^+$).

H_2L^4. Compounds **1** (2.00 g, 7.80 mmol) and **5** (2.47 g, 15.6 mmol) were added to dmf (40 cm^3) and stirred for 7.5 h at 40 °C under nitrogen. To the resulting orange slurry was added acetone (300 cm^3). The system was stirred for 15 min and then left to settle overnight. The crude product was isolated by filtration and washed with acetone (100 cm^3). After drying under vacuum, first at room temperature for 30 min and then at 150 °C for 8 h, a light peach-coloured solid was obtained. According to ^{1}H NMR results this crude product contained dmf as the only major impurity. In order to obtain a product free from dmf the crude product was recrystallised from water. After dissolution in boiling water (1800 cm^3) the yellow

solution was filtered and evaporated at boiling point until *ca.* 500 cm^3 remained (at which point recrystallisation commenced). After cooling on ice overnight, the recrystallised product was isolated, washed with water (40 cm^3) and acetone (20 cm^3) and finally dried under vacuum at 150 °C for 8 h. After drying, the trihydrate of H_2L^4 (1.65 g, 34% based on **1**) was obtained as a light brown powder, m.p. >350 °C (Found: C, 34.7; H, 4.6; N, 22.1; S, 10.0%; $M - H^+$ *m*/*z* 571. $C_{18}H_{24}N_{10}O_8S_2 \cdot 3H_2O$ requires C, 34.5; H, 4.8; N, 22.3; S, 10.2%; *M* 572). $\tilde{\nu}_{max}/cm^{-1}$ (CO) 1703vs; (amide I) 1622vs; (amide II) 1542m; (amide III) 1260m; (CS) 1189; δ_H(270 MHz) 2.98 (4 H, s, NCH_2CH_2N), 3.52 (4 H, s, NCH_2CO), 3.59 (4 H, s, NC$H_2$$CO_2$H), 6.35 (4 H, s, NH_2), 8.72 (2 H, s, NHCO), 11.8 [2 H, br s, C(NH_2)N*H*CS] and 11.99 (2 H, s, CSNHCO); δ_C(100 MHz) 51.9 (NCH_2CH_2N), 55.2 (NCH_2CONH), 57.2 (NC$H_2$$CO_2$H), 91.0 (uracil C5), 150.4 (uracil C6), 159.0 (uracil C2), 170.4 (uracil C4), 172.3 (NCH_2*C*ONH) and 173.0 (NCH_2*C*O_2H); *m*/*z* 597 ($M - H^+$). Attempts to recover more product from the yellow eluate from the final filtration only produced a small amount of an impure product.

Synthesis of the metal complexes

K[VO_2L^1]·5H_2O. Ammonium metavanadate (0.28 g, 2.39 mmol) was dissolved in aqueous 0.053 M KOH solution (48 cm^3) at room temperature. Once the solid had dissolved, water (200 cm^3) was added and the solution boiled for 20 min in an open flask, in order to drive off ammonia. After this stage 100 cm^3 of the solution remained. Next, H_2L^1 (1.17 g, 2.29 mmol) was added to the hot solution. The ligand rapidly dissolved, forming a yellow solution. The solution was refluxed for 25 min and then allowed to cool to room temperature. The first crystals formed (after standing overnight) were yellow needles of good enough quality for crystallography. More product was obtained by evaporating the solution until 20 cm^3 remained, and then leaving it for 2 weeks at room temperature in a sealed flask (the crystallisation of the product was extremely slow). The final product was isolated by filtration and left to dry on filter-paper at room temperature for several days. The salt K[VO_2L^1]·5H_2O loses its water of crystallisation at temperatures above 50 °C. Total yield: 0.89 g (52%), m.p. >350 °C (Found: 30.2; H, 4.1; N, 15.6. $C_{18}H_{30}KN_8O_{17}V$ requires C, 30.2; H, 4.0; N, 15.9%). $\tilde{\nu}_{max}/cm^{-1}$ (CO) 1708vs; (amide I) 1658vs; (amide II) 1552m; (amide III) 1241m; (VO) 921s and 894vs; δ_H(270 MHz) 2.64, 2.68, 2.93, 2.96 (all 1 H, s, NCH_2CH_2N), 3.38, 3.42, 3.63, 3.70 (all 1 H, s, CH_2CONH), 3.71, 3.77, 4.21, 4.28 (all 1 H, s C$H_2$$CO_2$H), 7.98 (2 H, s, uracil CH), 8.72 (2 H, s, NCH_2CO), 10.7 (2 H, br s, CHN*H*CO) and 11.4 (2 H, s, CONHCO); *m*/*z* 574 ($VOL^1 - H^+$) and 557 [$(VL^1)^+ - 2H^+$].

[Zn(OH_2)L^1]. The compound H_2L^1 (0.555 g, 1.07 mmol) and Zn(O_2CMe)$_2$·2H_2O (0.239 g, 1.30 mmol) were refluxed in water (100 cm^3) overnight. The cloudy solution was then cooled to room temperature and the crude product isolated by filtration and washed with water (2 × 30 cm^3). Recrystallisation was performed by dissolving the crude product in boiling water (600 cm^3), cooling it to room temperature and leaving it for several days (as in the case of K[VO_2L^1]·5H_2O, the recrystallisation was extremely slow). Finally, the hydrated product was isolated as a white microcrystalline mass by filtration and dried in an oven at 100 °C overnight. The drying destroyed the crystalline character (due to loss of water of crystallisation), and produced [Zn(OH_2)L^1] as a white, amorphous solid. Yield; 0.49 g (82%), m.p. >350 °C (Found: C, 36.4; H, 3.5; N, 18.8. $C_{18}H_{22}N_8O_{11}Zn$ requires: C, 36.5; H, 3.4; N, 18.9%). $\tilde{\nu}_{max}/cm^{-1}$ (CO) 1721vs and 1657vs; (amide I) 1636vs; (amide II) 1592m and 1553m; (amide III) 1241; δ_H(270 MHz) 2.61, 2.76, 2.84, 2.88 (all 1 H, s, NCH_2CH_2N), 3.06 (4 H, s, CH_2CONH), 3.39, 3.50, 3.67, 3.74 (all 1 H, s, C$H_2$$CO_2$H), 8.00 (2 H, d, ^3J 5.9, uracil CH), 9.79 (2 H, s, NCH_2CO), 10.79 (2 H, dd, ^3J 5.2, ^4J 1.3, CHN*H*CO) and 11.49 (2 H, d, ^4J 1.6 Hz, CONHCO).

[Zn(OH_2)L^1]·4H_2O. A small amount of recrystallised, dried [Zn(OH_2)L^1] was dissolved in the minimum amount of boiling water. After filtration, the flask containing the hot solution was allowed to cool very slowly to room temperature immersed in an oil-bath. The procedure produced colorless, prismatic single crystals of [Zn(OH_2)L^1]·4H_2O, some of which were good enough for crystallography (Found: C, 32.3; H, 4.5; N, 1.6. $C_{18}H_{30}N_8O_{15}Zn$ requires C, 32.6; H, 4.55; N, 16.9%).

[Zn(OH_2)L^3]·5H_2O. The compound H_2L^3 (0.135 g, 0.25 mmol) and Zn(O_2CMe)$_2$·2H_2O (0.060 g, 0.25 mmol) were refluxed in water (30 cm^3) for 4 h. The resulting yellow solution was cooled on ice. The crude, precipitated product was isolated by filtration, washed with water (15 cm^3) and redissolved in boiling water. Upon slow cooling of the solution in a sealed Dewar vessel for several days, colorless crystals of the target compound were obtained. Yield: 0.070 g (53%), m.p. >350 °C (Found: C, 30.2; H, 4.5; N, 19.6%; $M - H^+$ *m*/*z* 601. $C_{18}H_{34}N_{10}O_{16}Zn$ requires C, 30.4; H, 4.8; N, 19.7%; *M* 602). $\tilde{\nu}_{max}/cm^{-1}$ (CO) 1725vs; (amide I) 1637vs and 1604m; (amide II) 1540m; (amide III) 1265m; δ_H(270 MHz) 3.19 (4 H, s, NCH_2-CH_2N), 3.41 (4 H, s, NCH_2CO), 3.44 (4 H, s, NC$H_2$$CO_2$H), 6.34 (4 H, s, NH_2), 8.50 (2 H, s, amide NH), 10.40 [2 H, s, C(NH_2)N*H*CO] and 10.55 (2 H, s, CON*H*CO); *m*/*z* 601 ($M - H^+$).

[NiL^1]·3H_2O. Compound H_2L^1 (0.25 g, 4.8 mmol) was dissolved in aqueous 0.053 M KOH (19 cm^3). When all the ligand had dissolved, the solution was heated to 90 °C and a solution consisting of Ni(O_2CMe)$_2$·4H_2O (0.12 g, 4.8 mmol) in water (40 cm^3) was added dropwise [1 drop every second; a slow addition is crucial in order to avoid precipitation of Ni($OH)_2$]. The clear reaction mixture gradually turned blue, but when *ca.* 30 cm^3 of the acetate solution had been added precipitation of a blue solid suddenly occurred. When the addition was complete the light blue, extremely fine-grained solid was isolated by filtration from the colorless solution and dried in an oven at 65 °C for 4 d. It was found to be the trihydrate of the target complex [NiL^1] (Found: C, 34.6; H, 3.9; N, 17.8%; $M - H^+$ *m*/*z* 565. $C_{18}H_{26}N_8NiO_{13}$ requires C, 34.8; H, 4.2; N, 18.0%; *M* 566). $\tilde{\nu}_{max}/cm^{-1}$ (CO) 1717vs and 1680vs; (amide I) 1657vs and 1636vs; (amide II) 1597s; (amide III) 1264.

Crystallography

Table 4 provides a summary of the crystal data, data collection and refinement parameters for complexes K[VO_2L^1]·5H_2O, [Zn(OH_2)L^1]·4H_2O, and [Zn(OH_2)L^3]·5H_2O. The structures were solved by direct methods and all of the non-hydrogen atoms were refined anisotropically by full-matrix least squares based on F^2. In each structure the C–H hydrogen atoms were placed in calculated positions, assigned isotropic thermal parameters, $U(H) = 1.2U_{eq}(C)$, and allowed to ride on their parent atoms. The N–H and O–H hydrogen atoms in [Zn(OH_2)L^1]·4H_2O and [Zn(OH_2)L^3]·5H_2O were located from ΔF maps and refined isotropically subject to a distance constraint. In K[VO_2L^1]·5H_2O, however, they could not be located and so the N–H hydrogen atoms were placed in calculated positions, assigned isotropic thermal parameters, $U(H) = 1.2U_{eq}(N)$, and allowed to ride on their parent atoms; the O–H hydrogen atoms were not included. In the [Zn(OH_2)L^3]·5H_2O complex a solvent water (SWAT) correction was also applied. The largest difference peak of 1.1 electrons in [Zn(OH_2)L^1]·4H_2O is less than 1 Å away from the zinc centre (with the next highest peak being due to less than 0.6 electrons) and must be assigned to residual absorption effects. Though many different absorption corrections were tried, none succeeded in removing this peak. Computations were carried out using the SHELXTL PC program system.[10]

CCDC reference number 186/944.

Table 4 Crystal data, data collection and refinement parameters[a]

	$K[VO_2L^1]\cdot 5H_2O$	$[Zn(OH_2)L^1]\cdot 4H_2O$	$[Zn(OH_2)L^3]\cdot 5H_2O$
Formula	$C_{18}H_{20}KN_8O_{12}V\cdot 5H_2O$	$C_{18}H_{22}N_8O_{11}Zn\cdot 4H_2O$	$C_{18}H_{24}N_{10}O_{11}Zn\cdot 5H_2O$
M	720.5	663.9	711.9
Colour, habit	Pale yellow prisms	Clear prismatic blocks	Clear prisms
Crystal size/mm	0.30 × 0.20 × 0.17	0.27 × 0.17 × 0.17	0.13 × 0.13 × 0.12
Space group	$P2_1/n$ (no. 14)	$C2/c$ (no. 15)	$P2_1/c$ (no. 14)
T/K	293	293	203
a/Å	6.540(1)	11.475(2)	11.342(1)
b/Å	25.967(2)	9.709(1)	9.555(1)
c/Å	16.643(1)	22.620(2)	25.876(1)
β/°	91.72(1)	94.12(2)	95.58(1)
U/Å^3	2825.2(5)	2513.5(5)	2791.0(4)
Z	4	4[b]	4
D_c/g cm^{-3}	1.694	1.754	1.694
F(000)	1488	1376	1480
Radiation used	Cu-Kα	Cu-Kα	Cu-Kα[c]
μ/mm^{-1}	5.11	2.21	2.08
θ Range/°	3.2–60.0	3.9–63.7	3.4–60.0
No. of unique reflections measured	4205	2077	4149
observed, $\|F_o\| > 4\sigma(\|F_o\|)$	3514	1691	3198
Maximum, minimum transmission	0.15, 0.07	0.87, 0.47	0.78, 0.59
No. of variables	406	224	495
$R1$[d]	0.058	0.057	0.065
$wR2$[e]	0.166	0.134	0.162
Weighting factors a, b[f]	0.090, 2.777	0.090, 1.958	0.098, 6.027
Largest difference peak, hole/e Å^{-3}	0.72, −0.86	1.14, −0.58	0.88, −1.09

[a] Details in common: monoclinic; graphite-monochromated radiation, ω scans, Siemens P4 diffractometer, semiempirical absorption correction, refinement based on F^2. [b] The molecule has crystallographic C_2 symmetry. [c] Rotating-anode source. [d] $R1 = \Sigma\big||F_o| - |F_c|\big|/\Sigma|F_o|$. [e] $wR_2 = [\Sigma w(F_o^2 - F_c^2)^2/\Sigma w(F_o^2)^2]^{\frac{1}{2}}$. [f] $w^{-1} = \sigma^2(F_o^2) + (aP)^2 + bP$.

Acknowledgements

S. U. thanks the Swedish Natural Science Research Council (NFR) for a post-doctoral grant. BP plc is thanked for endowing D. M. P. M's chair.

References

1 J.-M. Lehn, *Angew. Chem., Int. Ed. Engl.*, 1988, **27**, 89; A. F. Williams, *Pure Appl. Chem.*, 1996, **68**, 1285; E. C. Constable, *Chem. Commun.*, 1997, 1073; R. Kramer, J.-M. Lehn and A. Marquis-Rigualt, *Proc. Natl. Acad. Sci. USA*, 1993, **90**, 5394.

2 A. D. Burrows, C.-W. Chan, M. M. Chowdhry, J. E. McGrady and D. M. P. Mingos, *Chem. Soc. Rev.*, 1995, **24**, 329; M. M. Chowdhry, D. M. P. Mingos, A. J. P. White and D. J. Williams, *Chem. Commun.*, 1996, 899; C.-W. Chan, D. M. P. Mingos, A. J. P. White and D. J. Williams, *Polyhedron*, 1996, **15**, 1173; *Chem. Commun.*, 1996, 81; J. E. McGrady and D. M. P. Mingos, *J. Chem. Soc., Perkin Trans. 2*, 1995, 2287; A. D. Burrows, D. M. P. Mingos, A. J. P. White and D. J. Williams, *J. Chem. Soc., Dalton Trans.*, 1996, 3805.

3 M. B. Inoue, M. Inoue, I. C. Munoz, M. A. Bruck and Q. Fernando, *Inorg. Chim. Acta*, 1993, **209**, 29; S. J. Franklin and K. N. Raymond, *Inorg. Chem.*, 1994, **33**, 5794.

4 M. S. Konings, W. C. Dow, D. B. Love, K. N. Raymond, S. C. Quay and S. M. Rocklage, *Inorg. Chem.*, 1990, **29**, 1488; F. Jasanada and F. Nepveu, *Tetrahedron Lett.*, 1992, **33**, 5745; L. Ehnebohm, B. F. Pedersen and J. Klaveness, *Acta Chem. Scand.*, 1993, **47**, 965; S. W. A. Bligh, A. H. M. S. Chowdhury, M. McPartlin, I. J. Scowen and R. A. Bulman, *Polyhedron*, 1995, **14**, 567.

5 D. Parker and J. A. G. Williams, *J. Chem. Soc., Dalton Trans.*, 1996, 3613.

6 D. J. Hnatowich, M. W. Layne and R. L. Childs, *Int. J. Appl. Radiat. Isot.*, 1982, **33**, 327; M. W. Brechbiel, O. A. Gansow, R. W. Atcher, J. Schlom, J. Esteban, D. E. Simpson and D. Colcer, *Inorg. Chem.*, 1986, **25**, 2772.

7 A. Houlton, D. M. P. Mingos and D. J. Williams, *J. Chem. Soc., Chem. Commun.*, 1994, 503.

8 W. R. Scheidt, R. Countryman and J. L. Hoard, *J. Am. Chem. Soc.*, 1971, **93**, 3878.

9 T. N. Polynova, T. V. Filippova, M. A. Porai-Koshits, V. K. Bel'skii, A. N. Sobolev and L. I. Myachina, *Koord. Khim.*, 1988, **14**, 405; T. F. Sysoeva, Z. A. Starikova, M. V. Leont'eva and N. M. Dyatiova, *Zh. Strukt. Khim.*, 1990, **31**, 140.

10 SHELXTL PC, version 5.03, Siemens Analytical X-Ray Instruments, Madison, WI, 1994.

Received 26*th January* 1998; *Paper* 8/00682B